Precipitation Pattern Formation in the Copper(II) Oxalate System with Gravity Flow and Axial Symmetry

A. Baker,[‡] Á. Tóth,[†] D. Horváth,[†] J. Walkush,[‡] A. S. Ali,[‡] W. Morgan,[§] Á. Kukovecz,[||] J. J. Pantaleone,[§] and J. Maselko*,[‡]

Department of Physical Chemistry, University of Szeged, Hungary, Chemistry Department, University of Alaska, Anchorage, Department of Physics and Astronomy, University of Alaska, Anchorage, Department of Applied and Environmental Chemistry, University of Szeged, Hungary

Received: January 26, 2009; Revised Manuscript Received: May 28, 2009

Chemical systems that are far from thermodynamic equilibrium may form complex temporal and spatiotemporal structures. In our paper, we present unusual precipitation patterns that have been observed in the system of Cu(II)-oxalate. Starting with a pellet of copper sulfate immersed in or by pumping copper sulfate solution into a horizontal layer of sodium oxalate solution, we have observed the formation of a precipitate ring and an array of radially oriented thin fingers. The development of these patterns is related to the internal structure of the different crystals, the gravity flow, and the circular symmetry of the experimental arrangement.

Introduction

Formation of crystals occurs on multiple levels. The position of atoms and molecules in crystals is defined by the crystallization structure (unit cell). As these basic cells grow, crystals with different shapes can be formed within the same lattice.[1,2] On a higher level, precipitation patterns evolve in which crystals are organized in space. These kinds of structures include Liesegang rings,[3−7] diffusion-limited aggregations[8,9] (DLA), snowflake formations,[10,11] chemical gardens,[12−18] hydrothermal vents,[19] and others.[20−22] Dendrites and snowflakes are formed in the process of crystallization in which, in addition to diffusion, important roles are played by the heat released during the crystallization and the curvature effect. These are described by the Mullins−Sekerka[23] instabilities. Similar complex structures may be obtained in the formation of fractal structures. These are modeled by DLA in which atoms or molecules diffuse to a seed, in which case the axial symmetry plays an important role. In the case of Liesegang rings, the layers of crystals are separated by layers of a clear solution. Experiments and calculations conducted by Ross[24,25] indicate that these structures can be described by Turing instabilities.[26] By changing system parameters or initial conditions, different complex patterns can be generated. The Liesegang experiments are performed in gel so that hydrodynamic motion can be excluded. The addition of hydrodynamics substantially increases the number of possible precipitation structures. Examples include precipitation patterns reported by Simoyi,[27,28] polymerization by Pojman,[29] geochemical structures by Ortoleva,[30] formation of stalactites,[31] and terraces and domes observed at geothermal hot springs.[32] The formation of patterns in chemical systems in which chemical reactions, diffusion, and horizontal convective motion of solution interact has been recently described as a reaction-diffusion-advective system and has been extensively studied.[33−35] One of these systems is the so-called DIFICI (differential flow-induced chemical instability), in which spatial structures are induced not by different diffusions but by the different flow rates of chemicals.

Another area of study of complex precipitation pattern formation with hydrodynamics is the so-called silicate garden, in which most structures are formed from an elastic gel. The influence of hydrodynamic flows can be used to control pattern formation, such as during the method of precipitation growth templated by a fluid jet.[36] Possible technological applications of controlled precipitation structures have also been reported.[37−39]

In this paper, we present a study of complex precipitation patterns with unusual geometry in the system of copper^{2+} oxalate for an experimental arrangement with axial symmetry. At various sodium oxalate concentrations, different copper oxalate complexes are expected to form:[40] CuC_2O_4, $Cu(C_2O_4)_2^{2-}$, and $Cu(HC_2O_4)^+$, among which the neutral CuC_2O_4 is insoluble in water. The precipitation processes are controlled by the gravity flow. This leads not only to the formation of a precipitate with two different morphologies but also to their spatial separation and, hence, to unusual spatial structure. A modeling study of the arising gravity current is also carried out to facilitate the understanding of the observed phenomenon.

Experimental Methods

Sodium oxalate solution (VWR) with concentration varied between 0.01 and 0.10 M and a volume of 100 and 500 mL was poured into a Petri dish 14 cm in diameter or into a square dish with 22-cm-long sides. Special care was taken to level the dish to produce symmetric fluid flow. A 1.0 g pellet of milled copper sulfate (VWR) approximately 1 cm in diameter and 0.4 cm high was prepared. In the experiments, either a single pellet was dropped, or copper sulfate solution was pumped from below,[18] into the center of the reaction vessel containing the sodium oxalate solution, which was then covered by a transparent plate to avoid evaporation. The experiments, carried out at 20 ± 1, °C were recorded and later analyzed quantitatively by an imaging system.

The temporal evolution of the precipitation was studied spectrophotometrically in a separate set of experiments. For the experiments, 1.0 mL of 0.10 M copper sulfate solution and 1.0

* Corresponding author. Fax +1-907-7864697.
[†] Department of Physical Chemistry, University of Szeged.
[‡] Chemistry Department, University of Alaska.
[§] Department of Physics and Astronomy, University of Alaska.
[||] Department of Applied and Environmental Chemistry, University of Szeged.

10.1021/jp9007703 CCC: $40.75
Published on Web 07/01/2009

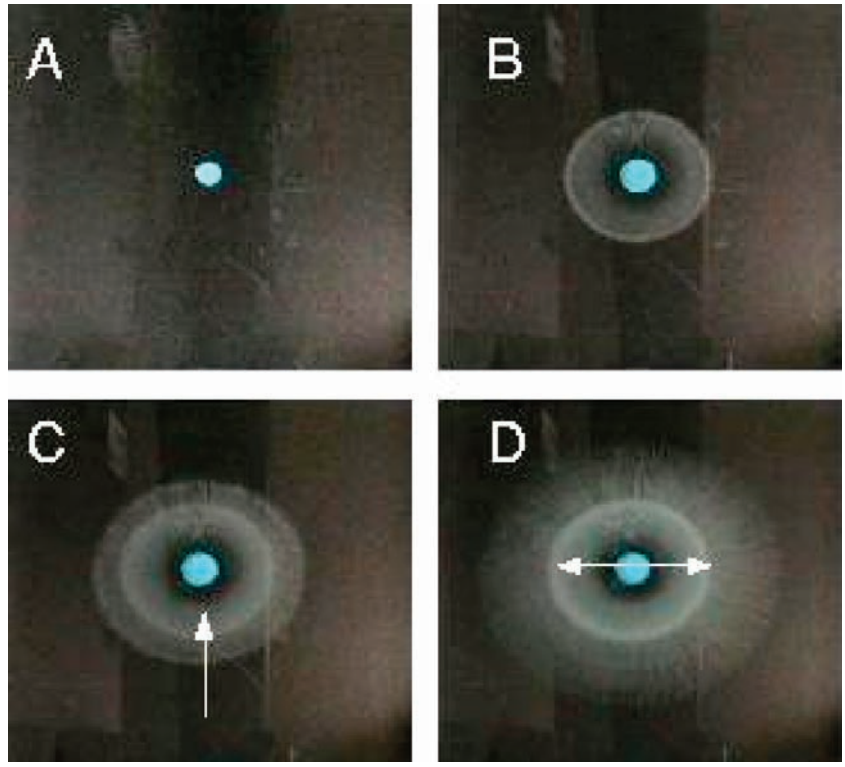

Figure 1. Temporal evolution of the precipitation in the form of ring and filaments around a copper sulfate pellet immersed in 0.03 M sodium oxalate solution at $t = 0$ s (A), 135 s (B), 270 s (C), 540 s (D). The arrow in part C illustrates the outer limit used to measure the initial transparent region; that in part D is the measured outer diameter of the precipitate ring.

mL of sodium oxalate solution were injected into a glass cuvette. The turbidity of the system was monitored by measuring the absorbance at 400 nm by a spectrophotometer (Varian, 50Bio). In addition, scanning electron microscope images were taken of the dried precipitate by a Hitachi S-4700 high-resolution scanning electron microscope.

Experimental Results

During the precipitation process, structures of unusual geometry evolve around the copper sulfate pellet or around the entrance where the copper sulfate solution is pumped in. No substantial differences have been found between the two configurations. In both cases, the precipitation leads to two distinct spatiotemporal patterns: a horizontally expanding precipitate ring and radially growing precipitate fingers.

After the pellet is submerged into the sodium oxalate solution, the copper sulfate starts to dissolve and the propagation of a precipitate front begins, as shown in Figure 1. As this white ring of precipitate with finely defined axial symmetry grows, it leaves behind an area of transparent solution without precipitate around the pellet. Quantitative analysis of the precipitation has been performed by measuring the radius of the transparent ring, the edge of which is indicated by the white arrow in Figure 1c, for oxalate concentrations varying between 0.02 and 0.10 M. It has been found that as the concentration of sodium oxalate increases, the transparent region shrinks, as illustrated in Figure 2a. Furthermore, this region entirely disappears as the oxalate concentration reaches 0.07 M. The maximum outer diameter reached by the precipitate ring, indicated by a white arrow in Figure 1d, has been found to be independent of the oxalate concentration under these experimental conditions, according to Figure 2b. Equivalent patterns are observed in experiments in which copper sulfate solution is pumped into the center instead of using a pellet.

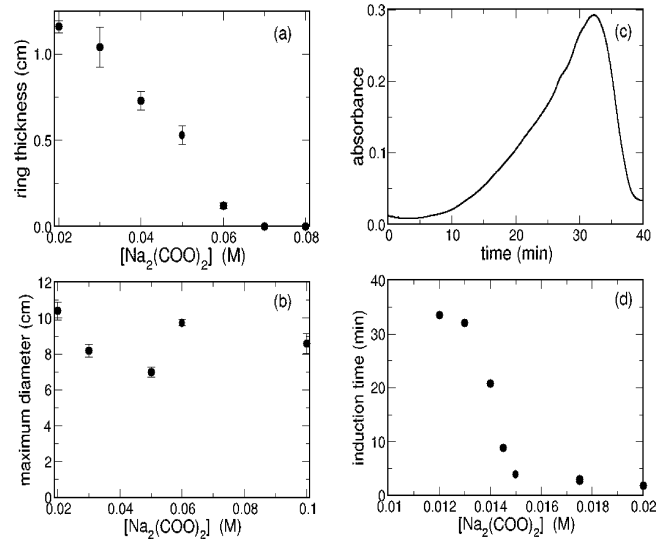

Figure 2. The ring thickness (radius) of the transparent regime (a) and the maximum diameter of the precipitate ring (b) as a function of sodium oxalate concentration. (c) Absorbance as a function of time for the precipitation reaction in the premixed system with $[CuSO_4] = 0.05$ M and $[Na_2C_2O_4] = 0.014$ M. (d) Induction time in the premixed system, measured as a time at which absorbance is greater than 0.2, as a function of oxalate concentration with $[CuSO_4] = 0.05$ M.

For oxalate concentrations between 0.02 and 0.1 M, many radially oriented delicate fingers appear concurrently to the precipitate ring and begin to grow (see the enlargement in Figure 3a). In experiments with a pellet in the center, the longest observed length of a finger was 25 cm, generally the order of the size of the container. In the beginning, the precipitate creating these fingers moves with the solution. This can be observed around the tip of the fingers where the fluid flow is apparently turbulent or upon shaking the container. As the

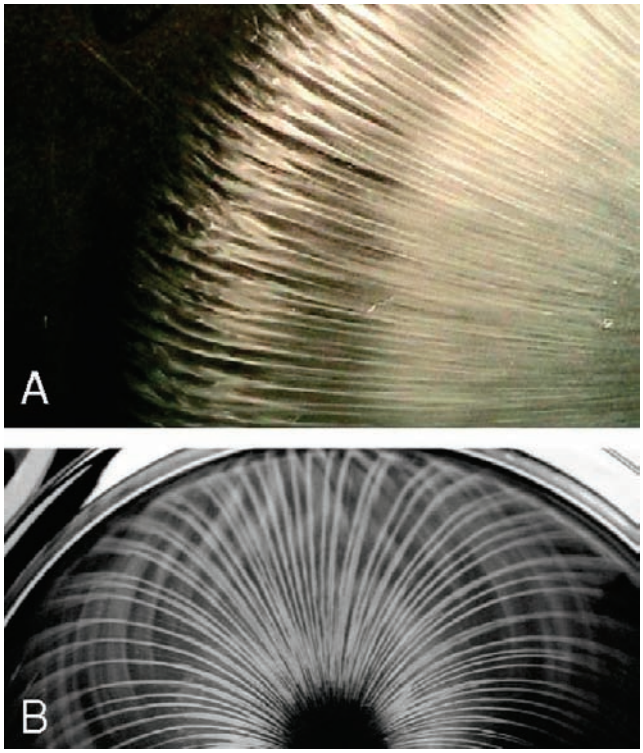

Figure 3. (A) The tip of filaments formed in 0.03 M sodium oxalate solution. The turbulent movement of precipitate is observed at the end of the delicate structures. (B) Reflection of growing fingers from the edge of the Petri dish in an off-centered experiment.

fingers grow, however, the precipitate particles settle, and about 1.5 cm from the tip, stick to the bottom, where they remain visible even after removing the solution. The fingers align themselves along the current; they may even exhibit reflection from the side of the container, as shown in Figure 3b for an asymmetric experiment with an off-centered pellet. The total number of fingers (200 ± 10) appears to be independent of flow rates and concentration of copper sulfate or sodium oxalate. In experiments in which the copper sulfate solution is pumped into the center, the length of fingers has been monitored as a function of time at various flow rates. As shown in Figure 4, the growth may be described by a power law with an exponent in the range of 0.52−0.55, slightly above the value for geometric spreading where the height of gravity current is assumed constant, in which case $r = a(wt)^{1/2}$ with system parameter a and flow rate w. According to Figure 5, a similar power law exists between the length reached at a given time and the flow rate.

Scanning electron microscopy images of the dried precipitate in the two distinct areas, the ring and the fingers, are presented in Figure 6. Crystals forming the precipitation ring are dominantly spherical in shape with a diameter of about 7 μm, whereas crystals forming the fingers have an elongated shape with a diameter of about 3 μm and a length on the millimeter scale. The latter crystals are oriented in the general direction of flow. By decreasing the oxalate concentration, the precipitation ring is not observed, and only fingers develop.

In our experiments, the sodium oxalate is in excess with respect to the copper sulfate;therefore, upon the complete dissolution of the pellet or after discontinuing the pumping, the entire precipitate dissolves in about 10−24 h, leading to a darker blue solution.

In a separate set of experiments, the two solutions, sodium oxalate and copper sulfate, were injected into a cuvette. Immediately upon mixing, the color of the solution turns deep blue, indicating the formation of a complex. Precipitation itself starts

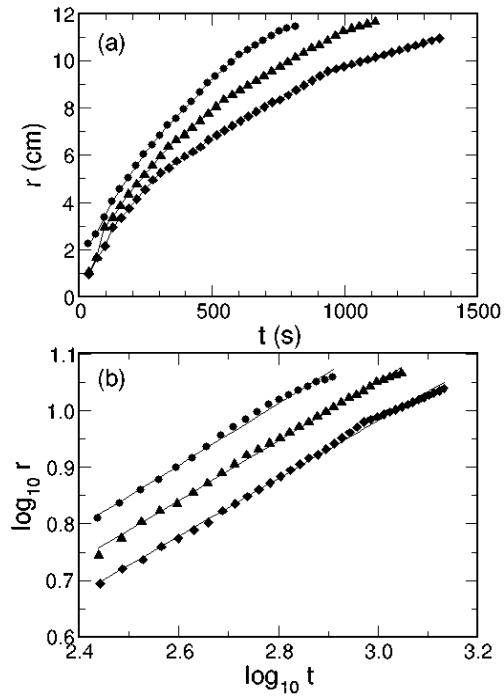

Figure 4. The temporal evolution of fingers (a) at flow rates 20, 15, 10 mL/h (from top to bottom). The slopes from the logarithmic plot (b) are 0.54 ± 0.01, 0.526 ± 0.005, and 0.511 ± 0.005 at the flow rates given.

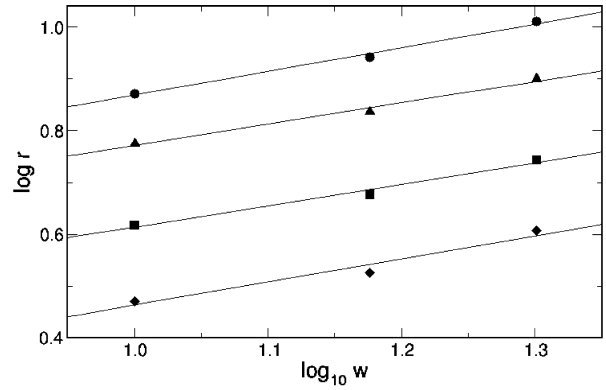

Figure 5. The power law dependence of filament length vs flow rate at times (from bottom up) of 120, 210, 390, and 600 s. The slopes are 0.45 ± 0.10, 0.41 ± 0.06, 0.41 ± 0.05, and 0.46 ± 0.04 in the given order.

only after an induction period of a few minutes. The turbidity of the solution can then be monitored by measuring the absorbance, which exhibits a bell-shape curve, as shown in Figure 2c. The increase in turbidity corresponds to the formation of the precipitate, whereas the decrease is a result of the sedimentation, during which the solution becomes transparent again. The induction time, defined as the time necessary for the absorbance to reach a value of 0.2, measured in a 1 cm cuvette, depends on the concentration of sodium oxalate, as presented in Figure 2d.

Modeling Study

When the copper sulfate pellet is immersed into the sodium oxalate solution, it starts to dissolve. The resultant solution layer containing copper sulfate has a higher density than the original solution; it therefore descends and spreads out along the bottom of the dish.[41] This outward flow of copper sulfate solution is driven by buoyant forces, and flows of this type are commonly called

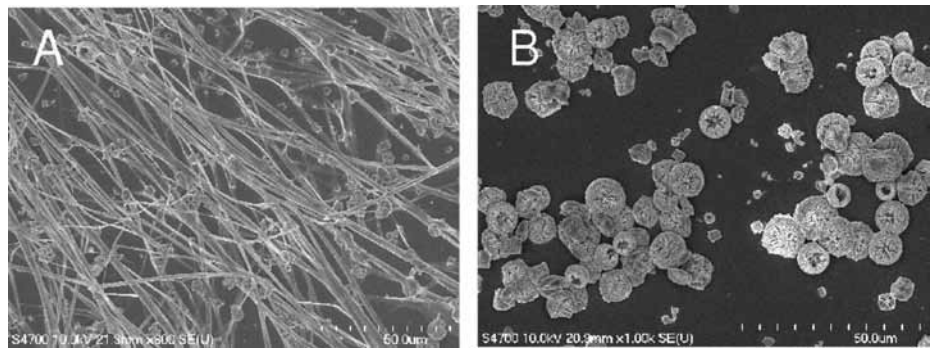

Figure 6. SEM images of the precipitate from the fingers (A) and from the ring (B). The field view corresponds to 100 μm.

gravity current. It is this gravity current along which the two solutions interact, leading to the formation of copper oxalate complexes and after some induction time to precipitation.

In our model, only the diffusion of copper sulfate salt from the pellet is considered in addition to the fluid flow; the effect of interfacial tension is thought to be negligible, since both fluids are aqueous and form a single phase.

The processes around the pellet are modeled numerically with a one-component system in cylindrical coordinates in which the hydrodynamics is governed by the Navier−Stokes equation with an incompressible fluid as

$$\frac{\partial C}{\partial t} = D\nabla^2 C - v\cdot\nabla C$$
$$\frac{\partial v}{\partial t} = \frac{\eta}{\rho_0}\nabla^2 v - v\cdot\nabla v - \frac{\nabla\rho}{\rho_0} - \frac{\rho}{\rho_0}g$$

where D is the diffusion coefficient of the solute and η is the dynamic viscosity of the solution. The density of the fluid is a function of the concentration as $\rho = \rho_0 + \rho_1 C$, with ρ_0 being the density of water. The system is essentially two-dimensional because the angular dependence is neglected due to the axial symmetry. To solve the equations in a cylindrical coordinate system with the gravitational field along the z-axis, we introduce dimensionless variables and consider the stream function-vorticity formalism. The concentration is scaled to that of the saturated solution as $c = C/C_0$, time scales according to $t \rightarrow (\eta/L_c^2\rho_0)t$, and velocity as $v \rightarrow (L_c\rho_0/\eta)v$ with the characteristic length, L_c, used also for the length scale. The stream function Ψ in our two-dimensional system is defined according to

$$v_r = \frac{-1\delta\psi}{r\delta z} \qquad v_z = \frac{1\delta\psi}{r\delta r}$$

The vorticity, $\omega = \nabla \times v$, at the same time eliminates the pressure term in the balance equation for momentum. The governing equations, hence, become

$$\frac{\delta c}{\delta t} = \frac{1}{\mathrm{Sc}}\left(\frac{\delta^2 c}{\delta r^2} + \frac{1}{r}\frac{\delta c}{\delta r} + \frac{\delta^2 c}{\delta r^2}\right) + \frac{1}{r}\left(\frac{\delta c}{\delta r}\frac{\delta\psi}{\delta z} - \frac{\delta c}{\delta z}\frac{\delta\psi}{\delta r}\right)$$
$$\frac{\delta\omega}{\delta t} = \left(\frac{\delta^2\omega}{\delta r^2} + \frac{1}{r}\frac{\delta\omega}{\delta r} + \frac{\delta^2\omega}{\delta z^2} - \frac{\omega}{r^2}\right) - \frac{\omega}{r^2}\frac{\delta\psi}{\delta z} + \frac{1}{r}\left(\frac{\delta\omega}{\delta r}\frac{\delta\psi}{\delta z} - \frac{\delta\omega}{\delta z}\frac{\delta\psi}{\delta r}\right) + \frac{\mathrm{Ra}}{\mathrm{Sc}}\frac{\delta c}{\delta t}$$
$$\omega = \frac{-1}{r}\left(\frac{\delta^2\psi}{\delta r^2} - \frac{1}{r}\frac{\delta\psi}{\delta r} + \frac{\delta^2\psi}{\delta z^2}\right)$$

where the Schmidt number is defined as $\mathrm{Sc} = \eta/(\rho_0 D)$ and the Rayleigh number as $\mathrm{Ra} = L_c^3\Delta\rho g/(\eta D)$ with $\Delta\rho$ representing the density difference between the saturated solution at the pellet and the fresh solvent.

In the calculations, L_c is set to 0.1 mm, which results in $\mathrm{Sc} = 500$ and $\mathrm{Ra} = 1000$. The equations are solved on a 400×100 grid with spacing 0.25 using an explicit Euler method for the initial value problem of c and ω with a time step of 0.0001 and a standard relaxation method for updating Ψ at each iteration step. For boundary conditions with respect to the velocity field we have free surface on the top and nonslip boundaries along the rest. For the concentration we have no-flux boundaries except at the lower left corner where we set $c = 1$ for 12 grid points at $r = 3$ to model the liquid layer at the surface of the pellet.

The solution with density greater than that of the surrounding fresh solvent corresponding to the solution layer at the pellet slips under the less dense liquid and at the same time forces it to flow upward. As the created vortex, an expanding torus in three dimensions, moves away from the left boundary, the gravity current spreads outward on the bottom of the liquid, as shown in Figure 7. Despite the diffusion of the solute into the fresh solvent, the denser liquid layer remains relatively thin because the vortex is located ahead of the tip of the gravity current, which results in the downward flow of fresh solvent from above the current. Inspection of the flow field presented in Figure 7 also reveals that turbulence and, hence, enhanced fluid mixing take place dominantly at the tip of the current.

The temporal evolution of the gravity current, monitored via the spreading of an isoconcentration line, may be approximated with a power law as shown in Figure 8. The obtained exponent (0.65) is slightly above that for simple geometric spreading.

Discussion

Formation of a Precipitation Ring. When the solution containing copper ions either from the dissolution of the pellet or from the external pumping comes into contact with the solution containing oxalate ions, an immediate complex formation occurs similarly to homogeneous mixtures, where it results in a color change to deeper blue. Although the neutral CuC_2O_4 form is insoluble, the precipitation reaction is slow, and it must overcome a nucleation barrier. The nucleation time depends on the concentration of ions and can be on the order of minutes for low oxalate concentration, as shown by the homogeneous experiments in the cuvette. In the Petri dish, the copper sulfate solution from the persistent dissolution or pumping therefore has time to spread out before precipitation occurs. In the applied concentration range, it has greater density than the sodium oxalate solution present in the dish; hence, it forms a visible

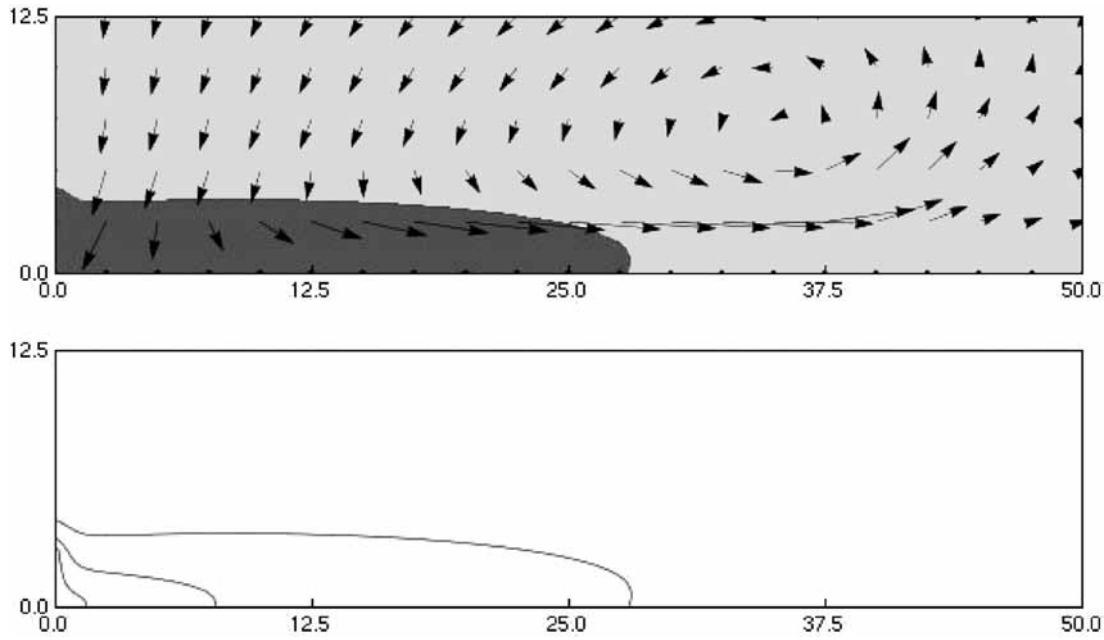

Figure 7. The calculated extent of the gravity current with the flow field (top) and with the location of the isoconcentration lines (0.5, 0.1, 0.01) (bottom) at $t = 3000$ dimensionless time.

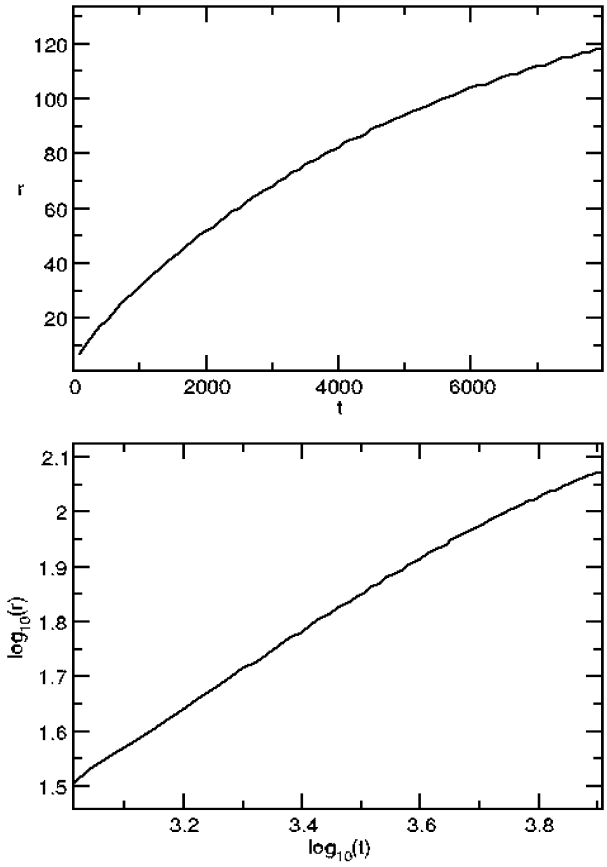

Figure 8. Progression of the gravity current measured by the advancement of the third isoconcentration line in Figure 6. (top) and the same in logarithmic plot (bottom).

gravity current with a height on the order of a millimeter by advancing on the bottom under the originally stationary liquid.

By increasing the oxalate concentration, the thickness of the transparent region around the pellet or the pump inlet decreases in accordance with the decrease in the induction time observed in the premixed system (cf. Figure 2). Hence, the origin of the transparent region without precipitate is related to the induction time necessary for the formation of copper oxalate precipitate.

The precipitate does not form a membrane that would separate the two solutions, as observed in various silicate solutions resulting in intriguing precipitate structures called chemical gardens. The spread of precipitate is associated with the outward flow of the dense solution containing copper sulfate; the obtained axial symmetry therefore simply reflects that of the source. The morphology of the precipitate abundant in this region, nodules with a diameter of 7 μm (see SEM image in Figure 5b) is typical for copper oxalate (CuC_2O_4).[42−44]

Formation of Fingers. In both experimental setups, the unusual spreading of the precipitate in the form of fingers is surprising. This unreported phenomenon is more dominant for small oxalate concentrations in which the formation of the circular precipitate ring is negligible. The experimental observations are supported by our model calculations of the hydrodynamics: the growth of fingers is governed by a gravity current of the dense copper sulfate solution, the spreading of which may be approximated with a power law.[45] The obtained SEM images reveal that the morphology of the precipitate is different (see Figure 6a): the fingers comprise filaments with typical dimensions of 3 μm diameter and up to 1 mm length. The filaments are generally oriented according to the growth direction of the finger, that is, parallel to the directaon of gravity current.

The spatial separation of the two forms of the precipitate suggests that the morphology of the insoluble particles plays an important role in the behavior with respect to the advection setup in the dish. The precipitate formed in the mixing zone of the two solutions, that is, above the gravity current, will both tend to be carried along with the surrounding fluid flow and, since having a greater density, settle out of the fluid with a terminal velocity, given for a solid, spherical nodule by

$$v_T = 2.7 \times 10^{-2}\ \text{mm/s}\ (d/7\mu)^2 \Delta\rho'/\rho$$

where d is the diameter of the nodule and $\Delta\rho'/\rho$ is the relative density difference between the precipitate and the fluid.

Similarly, the terminal velocity of a falling filament oriented horizontally to the flow is given by

$$v_T = 2.4 \times 10^{-2}\text{mm/s}\ (d/3\mu)^2 \Delta\rho'/\rho$$

where d is the diameter of the filament. According to Figure 6, the nodules have typical diameters about 7 μm, whereas filaments have diameters about 3 μm. The long length of the filament cancels out of the formula for the terminal velocity for both orientations. Thus, the two types of precipitate have approximately the same terminal velocity.

The maximum radius for the modulus, 4 cm (from Figure 2b), requires the nodules to be carried with the gravity current for, at most, ~150s (from Figure 4). Multiplying this time by the terminal velocity and assuming that $\Delta\rho'/\rho$ is on the order of 1, one gets the thickness of the gravity current to be about 1 to 2 mm. This thickness agrees with estimates of the flow thickness from diffusion. It is an interesting suggestion that the filaments have the same terminal velocity as nodules, yet are observed at much larger distances from the center.

For a gravity current flowing along a stationary bottom, it is common for vertical clefts to form in the head of the gravity current. This is because as the dense fluid flows, it tends to flow over some of the ambient fluid which sticks to the bottom. This creates a gravitational instability; the less dense fluid along the bottom will then tend to rise through the gravity current flow, producing a vertical cleft.[46−48] This mechanism may explain the formation of the fingers of copper oxalate precipitate. Figure 3a shows tips of growing fingers. The precipitation occurs in the lobes of the gravity current. The gravity current continues to flow even after precipitation is finished. This axi-symmetric outward flow means that the gravity current must expand angularly. We assume that the fibers are stuck together in tangles and, thus, are limited in how much they can expand angularly. Thus, the tangles move outward with widening gaps between them, producing the observed fingers pattern.

Conclusion

In this work, we have shown that the fluid flow arising from gravity current coupled by a precipitation reaction with considerable induction time leads to an unusual spatial distribution of the precipitate. In our system, copper oxalate precipitate with nodular morphology forms a ring around the pellet or inlet in accordance with the symmetry of the setup. In addition to the ring, radially growing thin fingers arise, comprising precipitate in the form of filaments, that represent a fingerprint of the flow pattern. The separation of fingers, that is, the breaking of circular symmetry, is brought about by the instability at the head of the gravity current.

The subject of copper oxalate nanostructures has become of interest lately.[49−51] Precipitation of copper and cobalt oxalate nanoparticles may lead to materials with giant magnetoresistance.[52] The formation of copper oxalate nanowires and copper nanostructures that can be obtained from the decomposition of copper oxalate has also been studied.[50,51] In our experiments, we have observed the formation of wires with a diameter of 0.3−3 μm and a length of a few millimeters. Application of hydrodynamic flow during crystallization process may be an efficient method to produce nanowires in copper oxalate or similar systems.

Acknowledgment. Discussions with Prof. Zoltán Rácz are gratefully acknowledged. This work was supported by the National Science Foundation (Grant no. CHE-0608631).

References and Notes

(1) Mann, S., Webb J., Williams R. J. P., Eds.; *Biomineralization: Chemical and Biochemical Perspectives*; VCH Publishers: Weinheim, 1989.
(2) Ozin, G.; Arsenault, A. *Nanochemistry*; RSC Publishing: Cambridge, 2005.
(3) Liesegang, R. *Naturwissenschaften* **1896**, *37*, 237.
(4) Kai, S.; Müller, S. C.; Ross, J. *J. Phys. Chem.* **1983**, *87*, 806.
(5) Rácz, Z. *Physica A* **1990**, *274*, 50.
(6) Hantz, P. *J. Phys. Chem. B* **2000**, *104*, 4266.
(7) Volford, A.; Izsák, F.; Ripszám, M.; Lagzi, I. *Langmuir* **2007**, *23*, 961.
(8) Nittmann, J.; Stanley, H. E. *Nature* **1986**, *321*, 663.
(9) Vicsek, T. *Fractal Growth Phenomena*; World Scientific: Singapore, 1989.
(10) Bentley, W. A.; Humphrey, W. J. *Snow Crystals*; Dover Publications Inc.: New York, 1962.
(11) Kikuchi, K.; Uyeda, H. *Atmos. Res.* **1998**, *47*, 169.
(12) Leduc, S. T. *The Mechanism of Life*; Rebman: New York, 1911.
(13) Collins, C.; Zhou, W.; Mackay, A.; Kalinowski, J. *Chem. Phys. Lett.* **1998**, *286*, 88.
(14) Coatman, R. D.; Thomas, N. L.; Double, D. D. *J. Mater. Sci.* **1980**, *15*, 2017.
(15) Cartwright, J. H. E.; Garcia-Ruiz, J. M.; Novella, M. L.; Otarola, F. *J. Colloid Interface Sci.* **2002**, *25*, 351.
(16) Thouvenel-Romans, S.; Steinbock, O. *J. Am. Chem. Soc.* **2003**, *125*, 4338.
(17) Thouvenel-Romans, S.; van Saarloos, W.; Steinbock, O. *Europhys. Lett.* **2004**, *67*, 42.
(18) Tóth, Á.; Horváth, D.; Smith, R.; McMahan, J. R.; Maselko, J. *J. Phys. Chem. C* **2007**, *111*, 14762.
(19) Boyce, A. J.; Coleman, M. L.; Russell, M. J. *Nature* **1983**, *300*, 545.
(20) Devon, R.; RoseFigura, J.; Douthat, D.; Kudenov, D.; Maselko, J. *Chem. Comm.* **2005**, *13*, 1678.
(21) San Ming, Y.; Sokolov, I.; Coombs, N.; Kresge, C.; Ozin, G. *Adv. Mater.* **1999**, *17*, 1427.
(22) Bensemann, I. T.; Fialkowski, M.; Grzybowski, B. A. *J. Phys. Chem. B* **2005**, *109*, 2774.
(23) Mullins, W.; Sekerka, R. *J. Appl. Phys.* **1963**, *34*, 323.
(24) Müller, S. C.; Kai, S.; Ross, J. *J. Chem. Phys.* **1982**, *86*, 4294.
(25) Ross, J.; Arkin, A. *J. Phys. Chem.* **1995**, *99*, 10417.
(26) Turing, A. *Philos. Trans. R. Soc. London B* **1952**, *237*, 37.
(27) Hauser, M. J. B.; Simoyi, R. H. *Phys. Lett. A* **1994**, *191*, 31.
(28) Martincingh, B. S.; Simoyi, R. H. *Phys. Rev. E* **1995**, *52*, 1606.
(29) Pojman, J. A. *J. Am. Chem. Soc.* **1991**, *113*, 6284.
(30) Ortoleva, P.; Chadam, J.; Merino, E.; Sen, A. *Am. J. Sci.* **1987**, *287*, 1008.
(31) Short, A.; Baygents, J.; Beck, J.; Stone, D.; Toomey, R., III; Goldstein, R. *Phys. Rev. Lett.* **2005**, *94*, 018501.
(32) Chen, P.; Goldenfeld, N. *Phys. Rev. E* **2007**, *76*, 046104.
(33) Rovinsky, A. B.; Menzinger, M. *Phys. Rev. Lett.* **1993**, *70*, 778.
(34) Andresen, P.; Bache, M.; Mosekilde, E.; Dewel, G.; Borckmans, P. *Phys Rev. E* **1999**, *60*, 297.
(35) Nekhamkina, O.; Sheintuch, M. *Phys. Rev. E* **2002**, *66*, 016204.
(36) Stone, D. A.; Lewellyn, B.; Baygents, J. C.; Goldstein, R. E. *Langmuir* **2005**, *21*, 10916.
(37) Maselko, J. *Material Sci. Eng., C* **1996**, *4*, 199.
(38) Mann, S. *Biomineralization Principles and Concepts in Bioinorganic Materials Chemistry*; Oxford Press: Oxford, 2001.
(39) Grzybowski, B. A.; Campbell, C. J. *Mater. Today* **2007**, *10*, 38.
(40) Marta, L.; Horovitz, O.; Zaharescu, M. *Leonardo J. Sci.* **2003**, *2*, 72.
(41) Maselko, J.; Geldenhuys, A.; Miller, J.; Atwood, D. *Chem. Phys. Lett.* **2003**, *373*, 563.
(42) Zhao, X.; Yu, J. *J. Cryst. Growth* **2007**, *306*, 366.
(43) Soare, L. C.; Bowen, P.; Lemaitre, J.; Hoffmann, H. *J. Phys. Chem. B* **2006**, *110*, 17763.
(44) Jongen, N.; Bowen, P.; Lemaitre, J.; Valmalette, J.-C. *J. Colloid Interface Sci.* **2000**, *226*, 789.
(45) Lemkert, C.; Imberg, J. *J. Hydraulic Eng. ASCE* **1993**, *119*, 662.
(46) Didden, N.; Maxworthy, T. *J. Fluid. Mech.* **1982**, *121*, 27.
(47) Huppert, H. E. *J. Fluid Mech.* **1982**, *121*, 43.
(48) Simpson, J. E. *J. Fluid Mech.* **1972**, *53*, 759.
(49) Li, M.-Y.; Dong, W.-S.; Liu, C.-L.; Lin, F.-Q. *J. Cryst. Growth* **2008**, *310*, 4028.
(50) Ahmad, T.; Chopra, R.; Ramanujachary, K. V.; Lofland, S. E.; Ganguli, A. K. *J. Nanosci. Nanotechnol.* **2005**, *5*, 1840.
(51) Soare, L. C.; Bowen, P.; Lamaitre, J.; Hofmann, H. *Mater. Res. Soc. Symp. Proc.* **2004**, *788*, 423.
(52) http://www.sbf.admin.ch / htm / dokumentation / publikationen/ international/cost/cd2006/cost/C99.0020.html (accessed June 18, 2009).

JP9007703